Paul R. Medwell, Qing N. Chan, Bassam B. Dally, Saleh Mahmoud, Zeyad T. Alwahabi, Graham J. Nathan

Temperature measurements in turbulent non-premixed flames by two-line atomic fluorescence

Proceedings of the Combustion Institute, 2013; 34(2):3619-3627

Temperature measurements in turbulent non-premixed flames by two-line atomic fluorescence

Paul R. Medwell[a,b], Qing N. Chan[a,b], Bassam B. Dally[a,b], Saleh Mahmoud[a,b], Zeyad T. Alwahabi[a,c], Graham J. Nathan[a,b]

[a] *Centre for Energy Technology,*
[b] *School of Mechanical Engineering, and*
[c] *School of Chemical Engineering, The University of Adelaide, S.A. 5005, AUSTRALIA*

Abstract

The temperature measured by non-linear excitation regime two-line atomic fluorescence, NTLAF, is compared with previous data in a well characterised turbulent non-premixed flame, known as the TNF DLR-A flame. The comparison of the previous detailed single-point measurements with the NTLAF measurements is used to assess the accuracy, and limitations, of the NTLAF technique. The NTLAF measurements were obtained using two different seeding methods, both separately and together, namely by seeding the indium as a solution of indium chloride conveyed as a fine mist with the fuel and by directly seeding neutral indium atoms into the fuel stream by laser ablation of an indium rod. Both instantaneous images and radial profiles of the mean and RMS data are reported for the different techniques. The calculated inter-pixel uncertainty of the measurements is estimated to be ∼50 K in the mean, and 8% uncertainty on an instantaneous basis. The comparison is performed on a conditional basis, given that the NTLAF measurements are limited to a lower temperature threshold and to the stoichiometric and rich regions of the flame. On this basis, the NTLAF method is found to generally agree with the TNF DLR-A data to within approximately 100 K.

Keywords: Temperature, Two-line atomic fluorescence (TLAF), Turbulent non-premixed flames

1. Introduction

Laser-based measurement techniques are established as the leading experimental research tool in turbulent reacting flows because of their unrivalled capacity to provide high temporal and spatial resolution, while also being able to target particular species [1]. Notwithstanding filtered Rayleigh scattering and NO LIF imaging (which both have limitations [2]) and the many other advances in laser diagnostic techniques, a planar technique providing well spatially resolved measurement of temperature is yet to be demonstrated in the reaction zone of turbulent sooty flames, which are encountered in many practical flames [3]. For example, Raman-Rayleigh scattering [4] is unable to provide measurements in the presence of the scattered interference from soot and its precursors, while Coherent Anti-stokes Raman Spectroscopy (CARS) [5] is limited to single point measurements [3]. Planar measurements are needed to resolve gradients in two dimensions, which control mixing rates in turbulent environments, and also to provide spatially correlated information about flow structure. A planar technique is also desirable to capitalise on other established planar techniques such as particle image velocimetry (PIV) for velocity, laser-induced incandescence (LII) for soot volume fraction and planar laser-induced fluorescence (PLIF) for OH and other species [3]. To this end, two-line atomic fluorescence (TLAF) has recently emerged as the technique with potential to provide planar measurement of temperature in turbulent flames containing soot [3]. To achieve high signal-to-noise ratio, the TLAF technique has been extended to operate beyond the linear excitation regime, which has been termed non-linear excitation regime TLAF (NTLAF) [2]. However, this is yet to be demonstrated in a turbulent environment. The overall aim of the present paper is therefore to demonstrate such a measurement.

The TLAF technique involves seeding into the flame a metal tracer, of which indium is the preferred species for thermometry [6] owing to its good sensitivity over the temperature range 800 to 2800 K [7, 8, 9]. The indium tracer is then excited from its neutral atomic state at two wavelengths, 410 nm and 450 nm, where interferences are less pronounced than in the UV range, and collected at 450 nm and 410 nm, respectively. This allows the signal to be separated from scattered interference, making it suitable for measurements in sooting flames [10]. It is also insensitive to collisional quenching [11]. For the seeding density selected in this study, attenuation was not observed. Furthermore, although beam steering is wavelength dependent, both

Stokes and anti-Stokes excitations are similar in wavelength. Thus any influences of attenuation and beam steering affect both images approximately equally, and have negligible effect on measurement accuracy. Early developments of the method were limited to low fluences, where the relationship between the excitation beam and the signal is linear. With some notable exceptions (*e.g.* [7]) linear-regime TLAF has been predominately limited to laminar flames. Extension to higher fluxes, where the relationship between the excitation beam and signal is non-linear, was developed by Medwell *et al.* [2] to allow single-shot measurements with and without the presence of soot. This has been termed non-linear excitation regime TLAF, or NTLAF, and has been demonstrated in both premixed and non-premixed flames [12]. Although operation in the non-linear excitation regime is susceptible to the effects of differing composition, the small amount of uncertainty associated with the determination of the constants is far outweighed by the ability to collect large dimension single-shot images with superior signal [2, 12]. More recently Chan *et al.* [13] demonstrated the simultaneous imaging of temperature with NTLAF and soot volume fraction by LII, with a reported measurement accuracy of $\sim$60 K. Nevertheless, all of these measurements have been performed in laminar (or wrinkled laminar) flames, where the seeding process is much simpler than in a turbulent flame. Since the concentration of any seeded species will decrease with distance from the nozzle, this will lead to a commensurate reduction in signal-to-noise ratio (SNR) with both axial distance from the nozzle and radial distance from the centre line. Hence the range of conditions over which useful measurements can be obtained in a turbulent flame is as yet unknown, as is the resolution of the measurement that can be achieved in practice. Finally, the indium marker is reactive, which not only limits its range of operation to fuel-rich conditions, but also raises questions as to the extent to which it will survive as a useful tracer in a turbulent environment. Hence, it is necessary to directly assess the range of conditions over which useful measurements can be obtained and the accuracy and uncertainty of the data.

A further issue has also arisen with the recent demonstration of laser ablation as a novel method to directly seed indium atoms at ambient temperature into a flow or flame [14]. This contrasts the seeding method reported previously, in which the indium was seeded into the flame as indium chloride dissolved in a solvent, and dispersed into the flame as small droplets. The requirement for a solvent using this approach will influence the flame temperature, either through heat of vapourisation or heat of combustion. A

comparison of solvents in the context of TLAF has been presented previously by Chan *et al.* [15], where it was shown that methanol provides the optimal signal (for the solvents considered). The ablation method therefore offers several potential advantages over the solvent-based seeding method. Not only does it avoid the need to evaporate the solvent, which may introduce local temperature gradients into the flame, but it also allows neutral indium to be detected at lower temperatures in the fuel-rich regions, which is not possible with nebuliser seeding that requires the reaction zone to initiate a conversion from the indium chloride salt [13]. In addition, the Stokes signal from the seeded indium has been shown to be a potential tracer for mixture fraction at ambient temperature [14, 16]. While further work is required to fully assess its accuracy as a scalar tracer at ambient conditions and to develop corrections for quenching at high temperature, even a qualitative marker will be useful. Nevertheless, the SNR of the ablation method is yet to be assessed in a turbulent environment. Hence, the recent development of the ablation seeding method for indium leads to the additional need to compare its effectiveness with that of the better established solvent-based method for the measurement of temperature in turbulent flames.

In light of the background described above, the aim of the present paper is to determine the range and accuracy over which NTLAF can provide measurements of temperature in a turbulent flame (i) by seeding with the established solvent-based method and/or by the new ablation method; and (ii) by direct comparison with established Raman-Rayleigh measurements in an identical flame. The chosen turbulent non-premixed flame for the comparison purposes of this study is the DLR-A flame [17]. Detailed data is available for this flame through the International Workshop on Measurement and Computation of Turbulent Non-premixed Flames (TNF) [18]. The NTLAF measurements are compared against the well-established TNF data to assess the accuracy and limitations of the NTLAF technique.

2. Experimental

2.1. Seeding System

Figure 1 shows a schematic diagram of the two types of seeding systems used to introduce indium into the flame. The fuel stream, which is also employed as the carrier gas for the indium, can be directed through either the nebuliser seeder or the ablation seeder. Alternatively, with both needle valves opened, the fuel flows simultaneously through both the nebuliser and

ablation seeders. The nebuliser method is operated with methanol as the solvent, because it has been demonstrated to yield the highest signal of the solvents considered [15]. The concentration of the methanol solution has been chosen to try and minimise any differences in adiabatic flame temperature (refer to §2.3).

The laser ablation method employs a pulsed and focused laser beam to remove metal from a surface by rapid heating, to release free atoms [19]. In addition, laser ablation also generates cations, anions, electrons, molecules, particles and particle clusters. In contrast to earlier work, which has generally been performed in low-pressure environments [20] with reduced collision rates, the present seeder operates at nominally atmospheric pressure.

The indium ablation system consists of a 10 mm diameter indium rod that is placed within an 'ablation chamber'. The rod is mounted on a motorized rotating shaft to provide a combined rotational and translational motion that exposes a "fresh" region of the rod to each ablating pulse. The rod was irradiated at 10 Hz by a focused, second harmonic output (532 nm) of a Q-switched Nd:YAG laser. The resulting ablation products were transported from the chamber by the fuel carrier gas, through a ballast volume with a motorized stirrer to damp the pulse-to-pulse variation in the generated indium, as a result of the pulsed ablation laser source. In addition, this arrangement generates velocities through the ballast volume that are sufficiently low to cause the larger particles to be removed by settling.

2.2. Optical Arrangement

The optical layout, shown schematically in Figure 2, consists of two distinct systems. The ablation seeding system utilises the 532 nm output from an Nd:YAG laser, in conjunction with beam steering and shaping optics to irradiate the indium rod within the ablation chamber to generate indium. The remainder of the optical system is dedicated to the generation of the laser pulses for indium fluorescence excitation and detection, namely at 410 and 450 nm.

The NTLAF process involves the Stokes ($5^2P_{1/2} \rightarrow 6^2S_{1/2}$) and anti-Stokes ($5^2P_{3/2} \rightarrow 6^2S_{1/2}$) excitation transitions, at 410nm and 450nm, respectively. Both the Stokes and anti-Stokes excitation beams are delivered at 3.5 mJ/pulse and combined into a co-planar sheet of 0.3 mm thickness and 12 mm height. The beams are directed through two glass slides and the diffuse scattering from the slides are directed through interference filters

onto a CCD camera to provide shot-to-shot corrections of spatial variations in the laser energy profile across the sheet height.

The fluorescence from the flame was detected through interference filters (10 nm bandwidth) by two intensified CCD (ICCD) cameras with f-number 1.4 lenses. The resultant images from the two cameras were spatially matched using a four-point matching algorithm and then morphed using an in-house cross-correlation algorithm to ensure sub-pixel matching and overlapping of the images. Determination of the temperature with the NTLAF technique requires calibration using a laminar premixed flame. For the present study, calibration constants were derived experimentally with a natural gas / air flame, seeded with indium using the ablation seeder. It has previously been shown that the calibration constants are independent of the fuel type and flame composition, within the uncertainty of the measurement [2, 12]. Further details on the optical arrangement are similar to those presented previously [2, 13]. No fluorescence was observed at any height when the seeders were switched off.

2.3. Burner Details

A simple jet burner is used to stabilise a previously reported turbulent jet non-premixed flame, DLR-A flame [17]. The burner consists of a 350 mm long straight stainless steel tube with an internal diameter of 8mm and a tapered end at the exit. The tube was placed at the centre of a co-flowing square jet of air with sides of 150mm, with an exit velocity of 0.5 m/s. The entire burner and co-flow system is translated axially through the fixed laser sheet to span the entire length of the flame.

The fuel composition for the flame was chosen to mimic the DLR-A mixture of 22.1% CH_4, 33.2% H_2, and 44.7% N_2 (by volume). In this study, natural gas was used instead of CH_4 so that small changes to the flowrates were required to compensate for the different composition. Specifically, the exit velocity of the present fuel jet was 42 m/s (*c.f.* 42.2 m/s), and the resultant Reynolds number was 15,750 (*c.f.* 15,200). Furthermore, when using the nebuliser seeding system, the addition of a small amount ($\lesssim$ 1% vol./vol.) of methanol into the fuel stream was also compensated by a small reduction in the flow rate of natural gas to maintain a fixed heat input. In both cases the visible flame length remained constant, while the jet momentum was within 1% of that reported by Meier *et al.* [17]. In addition the present co-flow velocity was introduced at 0.8 m/s, set by the lower limit of the fan, through a 150 mm square section nozzle, while the co-flow for the TNF DLR-A flame

measurements was introduced at 0.3 m/s through a 300mm square section nozzle.

3. Results and Discussion

3.1. Instantaneous Images

Figure 3 shows a series of typical raw (unprocessed) instantaneous indium fluorescence images at a range of heights above the jet exit plane (x/d), for the three seeding approaches. The Stokes image is on the left-hand side of the centreline, and the corresponding anti-Stokes image, which was collected simultaneously, is mirrored on the right-hand side. The images at each x/d are time independent, and are chosen to provide a direct comparison at each measurement height. Each image is 8 mm high and 32 mm wide. The colour-scale is constant for all images at each x/d and for all of the different seeding approaches.

Figure 3a presents the case where the indium is seeded in the form of indium chloride dissolved in methanol, with the use of the ultrasonic nebuliser. The signal-to-noise ratio (SNR) of the Stokes and anti-Stokes images are ∼15:1 and ∼5:1, respectively. The values for the SNR are approximately independent of x/d and are comparable with those reported previously in laminar flames [13]. This shows that, despite a ∼15-fold increase in the volumetric flowrate through the nebuliser seeding chamber, the same nebuliser seeding arrangement provides effective seeding for the turbulent flames considered in this study. Importantly, dilution of the seeded indium with the surrounding air at the downstream locations does not lead to a reduction in the absolute signal level. This observation suggests either that the indium atoms, once formed, tend to survive significant distances (and/or residence times), and in some cases, that neutral indium atoms may be generated within the flame, either by reduction of ions and/or from the vapourisation of solid particles.

Figure 3b shows the analogous series of typical raw (unprocessed) instantaneous indium fluorescence images for the case where the indium has been introduced into the flame with the ablation seeder. The colour-scale in Figure 3b is also constant at each x/d, and consistent with the images presented in Figure 3a. As with the nebuliser seeder, signal is observed at all measurement heights when using ablation seeding and, as with the nebuliser seeding, the values of the SNR are approximately independent of x/d. However, the SNR of the Stokes and anti-Stokes images is slightly lower at ∼12:1 and ∼3:1,

respectively, and the absolute signal intensity is also lower. Nonetheless, this reduction is attributed to the design of the respective seeders, rather than an inherent limitation of the ablation seeding technique. Furthermore, the ablation seeder has previously been demonstrated to have the advantage of signal in the unreacted regions of the flow [14] by generating stable indium atoms at ambient temperature and so avoiding the need to solvent evaporation. Worth noting, however, is that the intensity of the fluorescence in the unreacted region of the flow is lower than in the reaction zone, which is attributed to the generation of free indium atoms from other ablation products within the flame zone.

Figure 3c presents the corresponding series of typical raw (unprocessed) instantaneous indium fluorescence images for case with the indium introduced into the flame using both the nebuliser and ablation seeders simultaneously. This approach offers the advantages of both techniques. The SNR of the combined seeding is comparable to the nebuliser-only seeding (*viz.* ∼15:1 for Stokes and ∼5:1 for anti-Stokes) yet the total fluorescence intensity is increased. Most importantly, from Figure 3c it is determined that the two seeding approaches may be used concurrently without adversely affecting each other.

3.2. Temperature Profiles Deduced from Mean Images

The temperature has been calculated from the 500-shot ensemble averaged Stokes and anti-Stokes images. To avoid the influence on SNR of the low signal intensity values, a threshold was imposed to ensure that only pixels with an intensity corresponding to a temperature of 800 K were included in the calculations. The uncertainty in the temperature measurements is ∼50 K for each of the seeding techniques, and is primarily a result of laser energy correction uncertainty. It should be noted that calculating the temperature from the ensemble-averaged images can introduce a bias to the deduced temperature. The effect of this bias is highly dependent on the NTLAF calibration constants. For the measurements presented, the effect of this bias is within experimental uncertainty over the region of interest. The effect does, however, become more pronounced towards the boundaries of the measurement region, where other factors also reduce the measurement accuracy.

The mean NTLAF measurement radial profiles at x/d = 5, 10, 20 and 40 for each of the various seeding techniques are shown in Figure 4. In interpreting these results it is important to recall the conditional nature of the

method. Firstly, the NTLAF method has a minimum temperature threshold of 800 K, which results from the anti-Stokes ground-state Boltzmann fraction being $\lesssim$3% at this temperature. Furthermore, the surrounding air co-flow was not seeded because indium has been found not to survive far into the lean side of a reaction zone [15]. However, the indium is not completely consumed at the local stoichiometric contour, so that some indium fluorescence will be generated from the lean side. Hence, while the conditional requirement that $T \geq 800$ K can be strictly applied for both measurement techniques, the condition on mixture fraction is only approximately $\xi \geq \xi_{st}$ for the NTLAF measurement, while it has been applied strictly for the processing of the DLR-A dataset.

In each of the mean radial profile figures (Figure 4) both the unconditional mean temperature and a conditional mean measurement from the TNF DLR-A dataset has also been presented. The unconditional mean has been calculated from all of the available temperature points, while the conditional average has also been calculated for the TNF DLR-A dataset, from those points where $T \geq 800$ K and $\xi \geq \xi_{st}$. Since these conditions will reduce the number of available data points available from the TNF DLR-A dataset, a further limit is placed on the values used to determine the conditional average — namely there must be a minimum of 30 valid data points to be displayed in the radial profile to avoid the influence of intermittent data values.

Figure 4 shows that, on the rich-side of the flame, both the conditional and unconditional mean temperature for the TNF DLR-A dataset have very similar profiles. Thus, in this region, the conditional mean is insensitive to the exact thresholds chosen for the conditioning process, making this region ideal for comparing the two methods. Significantly, this region is also of greatest interest in the study of flames containing soot. Comparison of the NTLAF measurements with the conditional average from the TNF DLR-A dataset shows good agreement in general, particularly for $x/d \leq 10$. At these locations, the typical agreement is better than 50 K over the range of interest. It is only nearer the lower temperature limit where more significant variations occur — though these typically remain $\lesssim$100 K. On the lean side of the flame the unconditional data is consistently lower than the conditional data, as is expected due to the presence of cold ambient air. Similarly, at $x/d = 40$, the agreement between the NTLAF measurements and the TNF DLR-A data are within 100 K, with the best agreement found for the ablation seeder and the greatest differences on the fuel-rich side, close to the axis.

At the location $x/d = 20$, there is good agreement between the ablation-

seeded NTLAF measurements and the TNF DLR-A data set in the high temperature region of the flame, corresponding to $r/d \geq 1$. The disagreement in the central core is considered to be attributable to the differences in operating conditions between the present flame and DLR flame, notably to the substitution of methane with natural gas, the slightly lower jet velocity, the significantly higher co-flow velocity and the much smaller dimension of the co-flow nozzle. The height of $x/d = 20$ corresponds to the region of interaction between the end of the potential core of the co-flow jet and the flame for our case, while this region is further downstream for the TNF DLR-A flame measurements. In addition, at this height, the radial profiles are strongly sensitive to axial height, owing to the convergence of the flame from the outer to the central regions of the flame. This sensitivity contrasts to the much flatter profiles further downstream, at $x/d = 40$, where good agreement is found.

The final point to note is that the NTLAF measurements obtained with the nebuliser seeder are somewhat lower than those obtained by the ablation seeder in several regions of the flame. For example, it is $\sim$250 K lower at $x/d = 40$. It is possible that the latent heat of vaporisation of the methanol may be a contributing factor, but this is not expected to be the main cause.

3.3. Temperature Profiles from Instantaneous Images

Figure 5 presents the radial temperature profiles, where the NTLAF data have been calculated from each of the 500 instantaneous Stokes and anti-Stokes image pairs and with a higher temperature threshold of 1200 K in the conditional mean data. (In contrast, the data in Figure 4 were calculated from the ensemble mean images.) The higher threshold used here was chosen to reduce the inter-pixel noise, and corresponds to an anti-Stokes threshold of 30% of the peak signal. The uncertainty in the temperature images (as determined from the inter-pixel noise) is approximately 8%. In contrast, the lower threshold of 800 K, which equates to 10% of the peak anti-Stokes signal, was found to be too prone to extraneous noise on a single-shot basis. It should be noted that improvements with the seeding and optical system could improve the SNR, and enable a lower temperature limit.

Figure 5 includes the NTLAF results for the combined ablation and nebuliser seeding technique. Only a single technique is presented for a clear comparison of the NTLAF and TNF DLR-A datasets. The combined seeding approach yields the strongest signal, and has already been shown to give

similar results to the other seeding techniques, as presented in Figure 4. Other techniques show similar results to those presented in Figure 5.

Comparison with the conditionally averaged TNF DLR-A dataset reveals excellent agreement at $x/d = 5$ and 10. The agreement with the conditional mean and the RMS profiles is excellent over the range presented, and better than that obtained with the ensemble-averaged data and 800 K threshold (Figure 4). Radial profiles at $x/d = 20$ and 40 (not included for brevity) show similar differences between the NTLAF and the TNF DLR-A datasets as were observed in Figure 4, as reported in §3.2. That is, the TNF data are increasingly lower than the NTLAF data as the radial profile approaches the centre line at this downstream location, while that at $x/d = 40$, the agreement is better, with the NTLAF measurements being consistently lower.

A slight difference between the NTLAF data points and the TNF DLR-A dataset is found closest to the jet centreline. This is consistent with the trends observed in §3.2. Although the temperature threshold was set at 1200 K, the lowest mean temperature from NTLAF in Figure 5 is ∼1500 K. This difference is attributed to a combination of the threshold imposed on the anti-Stokes image (such that pixels with low signal intensity are discarded), and also the limitation that only data points are shown where there are greater than 30 samples.

4. Conclusions

The comparison of the NTLAF measurements with the previous TNF DLR-A measurements provides a means of assessing the accuracy of the NTLAF technique and supports the conclusion that the NTLAF method provides reliable measurements of temperature in a turbulent, non-premixed flame within its range of applicability. However, given that the technique is conditional on both a lower temperature threshold and on the instantaneous mixture fraction, care must be taken in interpreting the data.

In general, the NTLAF method was found to agree very well with the TNF data, and to be everywhere within 100 K except for the region near to $x/d = 20$, where the differences are attributable to differences in the dimensions of the co-flow nozzle and to slight differences in velocities and composition. It is notable that the agreement was excellent in the high temperature regions of the flame, near to stoichiometric.

The temperature measurements obtained with NTLAF by ablation seeding and by seeding with the nebuliser were found to exhibit good agreement

close to the burner in the regions of the flame close to stoichiometric. However, away from the near-stoichiometric zone and in the regions further downstream, the temperature measured with the nebuliser is $\sim$250 K lower than that with the ablator, which in turn yields better agreement with the TNF data. Since the calibration was performed with the ablation seeder, this suggests that the calibration may be sensitive to the method of seeding. Both seeding techniques, either separately or in combination, resulted in reasonable signal at all measurement locations above the burner. The SNR for the Stokes and anti-Stokes signals were found to vary slightly with the seeding technique, and to be in the order of 15:1 and 5:1, respectively.

Finally, a threshold was found in which the inter-pixel noise is sufficiently low to allow accurate measurements from the instantaneous images. For the present technique, this threshold was found to be 1200 K, but further developments in the seeding method are expected to allow this threshold to be lowered. This demonstration of the method paves the way for future application of the technique in the presence of soot, droplets and particulate fuels.

Acknowledgements

The authors wish to acknowledge the support of the Centre for Energy Technology and The University of Adelaide. The Australian Research Council is also gratefully acknowledged for their funding support of this work through ARC Discovery and LIEF grant schemes.

References

[1] K. Kohse-Höinghaus, R. S. Barlow, M. Aldén, J. Wolfrum, Combustion at the focus: laser diagnostics and control, Proceedings of the Combustion Institute 30 (2005) 89–123.

[2] P. R. Medwell, Q. N. Chan, P. A. M. Kalt, Z. T. Alwahabi, B. B. Dally, G. J. Nathan, Development of temperature imaging using two-line atomic fluorescence, Applied Optics 48 (6) (2009) 1237–1248.

[3] G. J. Nathan, P. A. M. Kalt, Z. T. Alwahabi, B. B. Dally, P. R. Medwell, Q. N. Chan, Recent advances in the measurement of strongly radiating, turbulent reacting flows, Progress in Energy and Combustion Science 38 (2012) 41–61.

[4] R. S. Barlow, Laser diagnostics and their interplay with computations to understand turbulent combustion, Proceedings of the Combustion Institute 31 (2007) 49–75.

[5] S. Roy, P. J. Kinnius, R. P. Lucht, J. P. Gord, Temperature measurements in reacting flows by time-resolved femtosecond coherent anti-Stokes Raman scattering (fs-CARS) spectroscopy, Optics Communications 281 (2008) 319–325.

[6] H. Haraguchi, B. Smith, S. Weeks, D. J. Johnson, J. D. Winefordner, Measurement of small volume flame temperatures by the two-line atomic fluorescence method, Applied Spectroscopy 31 (1977) 156–163.

[7] C. F. Kaminski, J. Engström, M. Aldén, Quasi-instantaneous two-dimensional temperature measurements in a spark ignition engine using 2-line atomic fluorescence, Proceedings of the Combustion Institute 27 (1998) 85–93.

[8] J. Engström, J. Nygren, M. Aldén, C. F. Kaminski, Two-line atomic fluorescence as a temperature probe for highly sooting flames, Optics Letters 25 (19) (2000) 1469–1471.

[9] J. Nygren, J. Engström, J. Walewski, C. F. Kaminski, M. Aldén, Applications and evaluation of two-line atomic LIF thermometry in sooting combustion environments, Measurement Science and Technology 12 (2001) 1294–1303.

[10] I. S. Burns, X. Mercier, M. Wartel, R. S. M. Chrystie, J. Hult, C. F. Kaminski, A method for performing high accuracy temperature measurements in low-pressure sooting flames using two-line atomic fluorescence, Proceedings of the Combustion Institute 33 (2011) 799–806.

[11] R. G. Joklik, J. W. Daily, Two-line atomic fluorescence temperature measurement in flames: an experimental study, Applied Optics 21 (22) (1982) 4158–4162.

[12] P. R. Medwell, Q. N. Chan, P. A. M. Kalt, Z. T. Alwahabi, B. B. Dally, G. J. Nathan, Instantaneous temperature imaging of diffusion flames using two-line atomic fluorescence, Applied Spectroscopy 64 (2) (2010) 173–176.

[13] Q. N. Chan, P. R. Medwell, P. A. M. Kalt, Z. T. Alwahabi, B. B. Dally, G. J. Nathan, Simultaneous imaging of temperature and soot volume fraction, Proceedings of the Combustion Institute 33 (2011) 791–798.

[14] P. R. Medwell, Q. N. Chan, B. B. Dally, Z. T. Alwahabi, S. Mahmoud, G. F. Metha, G. J. Nathan, Flow seeding with elemental metal species via an optical method, Applied Physics B: Rapid Communications, accepted 18th April, 2012.

[15] Q. N. Chan, P. R. Medwell, P. A. M. Kalt, Z. T. Alwahabi, B. B. Dally, G. J. Nathan, Solvent effects on two-line atomic fluorescence (TLAF) of indium, Applied Optics 49 (8) (2010) 1257–1266.

[16] Q. N. Chan, P. R. Medwell, B. B. Dally, Z. T. Alwahabi, G. J. Nathan, New seeding methodology for gas concentration measurement, Applied Spectroscopy, accepted 30th March, 2012.

[17] W. Meier, R. S. Barlow, Y.-L. Chen, J.-Y. Chen, Raman/Rayleigh/LIF Measurements in a Turbulent $CH_4/H_2/N_2$ Jet Diffusion Flame: Experimental Techniques and Turbulence-Chemistry Interaction, Combustion and Flame 123 (2000) 326–343.

[18] http://www.sandia.gov/TNF/DataArch/DLRflames.html, Last accessed: 26th December, 2011.

[19] J. S. Bakos, I. B. Földes, P. N. Ignácz, G. Kocsis, J. Szigeti, J. Kovács, Absolute measurement of velocity distribution of neutrals in sodium laser blow-off beam, Optics Communications 74 (1990) 374–379.

[20] S. Preuss, A. Demchuk, M. Stuke, Sub-picosecond UV laser ablation of metals, Applied Physics A 61 (1995) 33–37.

List of Figures

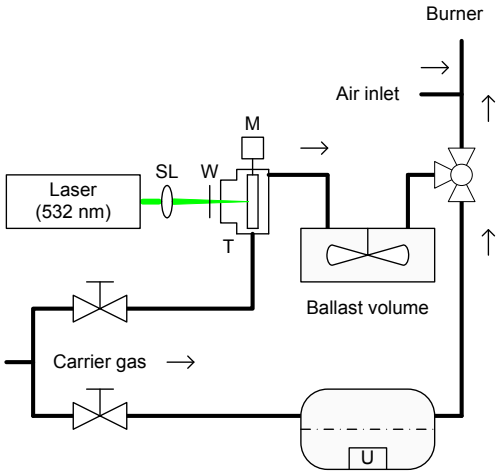

Figure 1: Schematic diagram of the seeding system. M, motor; SL, spherical lens; T, ablation target (indium rod); U, ultrasonic nebuliser; W, window.

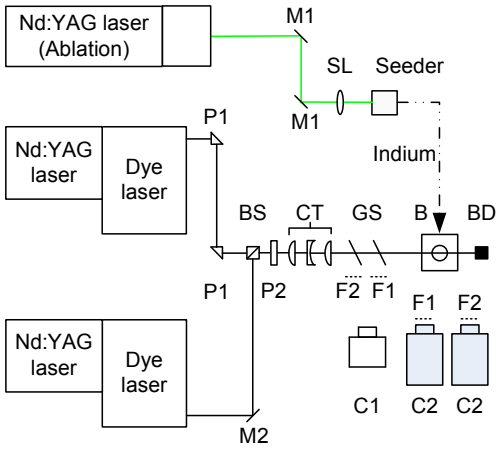

Figure 2: Schematic diagram of the optical arrangement. B, burner; BD, beam dump; C, camera; CT, cylindrical telescope; F, optical filter; GS, glass slide; M, mirror; P1, prism; P2, circular polariser; SL, spherical lens.

(a) Nebuliser Seeding

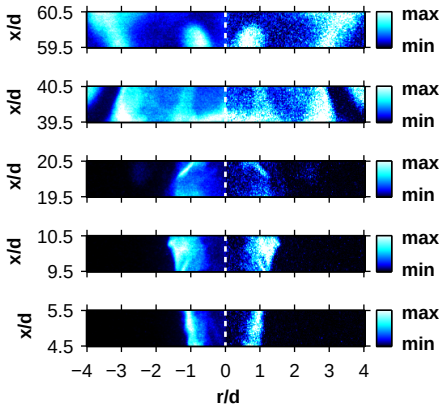

(b) Ablation Seeding

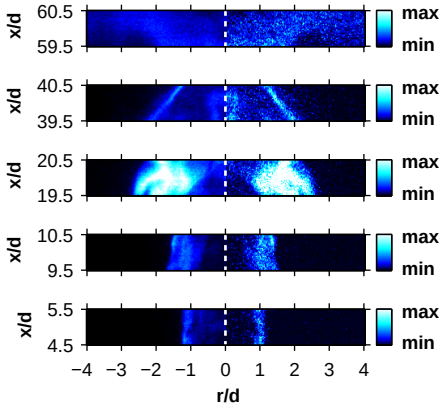

(c) Combined Seeding

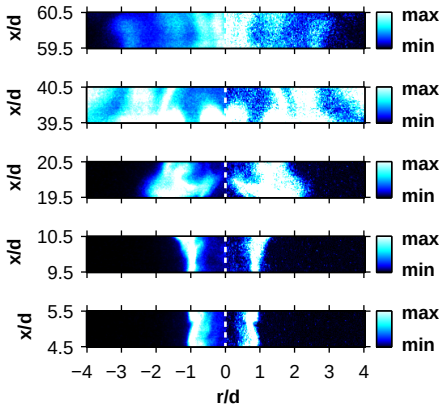

Figure 3: Sample raw instantaneous indium fluorescence images in the DLR-A flame, with (a) nebuliser seeding (b) ablation seeding and (c) combined ablation and nebuliser seeding. Left-hand and right-hand side of centreline (vertical dashed line) are Stokes and anti-Stokes images, respectively. Images at each x/d are time independent, and all images have the same constant colour-scale.

(a) $x/d = 40$

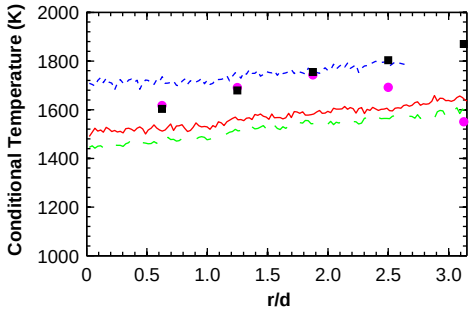

(b) $x/d = 20$

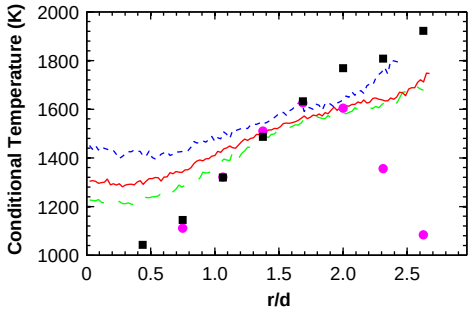

(b) $x/d = 10$

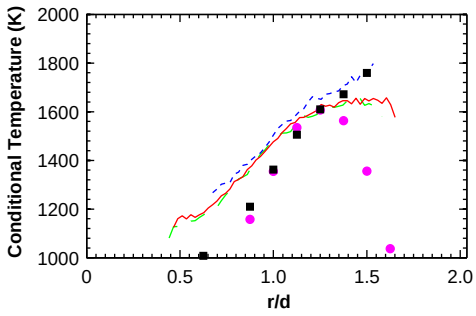

(c) $x/d = 5$

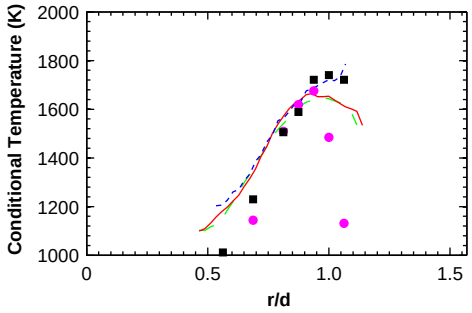

Figure 4: Mean radial temperature profiles of the DLR-A flame calculated from the mean of 500 image pairs for three seeding methods at (a) $x/d = 40$, (b) $x/d = 20$, (c) $x/d = 10$, and (d) $x/d = 5$. *Blue dotted line*: mean NTLAF measurements for ablation seeding. *Green dashed line*: mean NTLAF measurements for nebuliser seeding. *Red solid line*: mean NTLAF measurements for combined ablation and nebuliser seeding. *Magenta dots*: unconditional mean temperature from TNF DLR-A dataset. *Black squares*: conditional mean temperature from TNF DLR-A dataset, where $T \geq 800\ K$ and $\xi \geq \xi_{st}$.

(a) $x/d = 10$

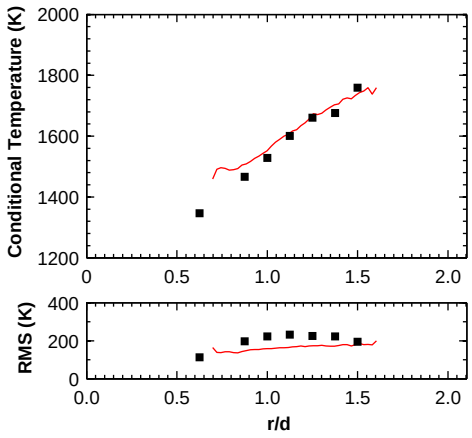

(b) $x/d = 5$

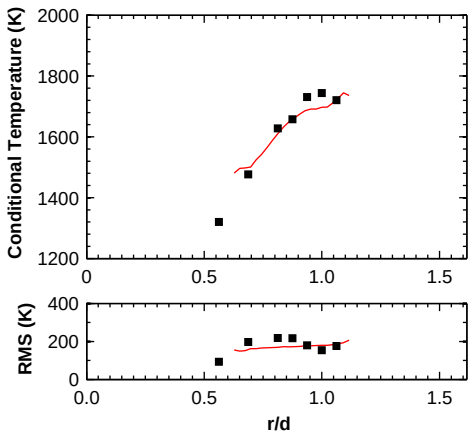

Figure 5: Mean and RMS radial temperature profiles for the DLR-A flame calculated from each instantaneous image pair for the combined ablation and nebuliser seeding, at (a) $x/d = 10$, and (b) $x/d = 5$. *Red solid line*: mean NTLAF measurements. *Black squares*: conditional mean temperature from TNF DLR-A dataset, where $T \geq 1200\ K$ and $\xi \geq \xi_{st}$.